1991

Large-aperture BVRJK photometry of rich abell clusters: constraints on dark matter

Stephen P. Boughn
Haverford College, sboughn@haverford.edu

J. M. Uson

THE ASTROPHYSICAL JOURNAL, 369:38–45, 1991 March 1

LARGE-APERTURE *BVRJK* PHOTOMETRY OF RICH ABELL CLUSTERS: CONSTRAINTS ON DARK MATTER

JUAN M. USON[1]
National Radio Astronomy Observatory,[2] P.O. Box O, Socorro, NM 87801
AND
STEPHEN P. BOUGHN[1]
Department of Astronomy, Haverford College, Haverford, PA 19041
Received 1990 June 25; accepted 1990 August 22

ABSTRACT

We present results of large (1′), single-aperture *JK* photometry and CCD *BVR* photometry on and near the centers of distant ($0.14 \leq Z \leq 0.20$), rich Abell clusters. The colors of the integrated light of the cores of these clusters are consistent with those of nearby E and S0 galaxies. The absence of anomalous infrared emission provides the strongest constraint to date on the possible stellar make-up of the dark matter in clusters of galaxies, requiring *K* band (2.2. μm) mass-to-light ratios of the dark matter of $(M/L)_K \geq 400h$. Indeed, no more than $5h^{-1}\%$ of the dark mass can be made of objects with mass greater than 0.1 $M_\odot$. Although these results do not require a contribution of nonbaryonic matter they provide some constraints on the mass function for baryonic objects which might compose the dark matter. These conclusions do not depend on the detailed distribution of the dark matter in the clusters.

Subject headings: cosmology — dark matter — galaxies: clusters — galaxies: photometry

1. INTRODUCTION

The mass required to gravitationally bind clusters of galaxies can be estimated from measurements of the velocity dispersions of the member galaxies and from the spectra of the X-ray emission from the intergalactic plasma. The derived masses often exceed the total mass in stars by two orders of magnitude (Faber & Gallagher 1979)—this is the well-known "dark matter" problem first noticed by Zwicky (1933). Often the mass of the X-ray emitting gas exceeds that of the stars (Henriksen & Mushotzky 1985; Sarazin 1986) but still falls short of that required to bind the cluster.

If this dark matter includes a stellar population which is distinct from that of normal galaxies, the colors of the integrated light from galaxy clusters would be different from those of normal galaxies. Since the infrared colors of galaxies (e.g., $V-K$ and $J-K$) are not very sensitive to absolute magnitude and morphological type (Aaronson 1977), they serve as excellent indicators of a distinct stellar population associated with the dark matter. For example, if the dark matter in a rich cluster, such as Coma, was in the form of the faintest known stars (e.g., VB10 which has $M_V = 18.9$ and $V-K = 9.0$; Greenstein, Neugebauer, & Becklin 1970) their integrated *K*-band luminosity would be comparable to that of the visible galaxies while they would be virtually invisible in the *V* band. The result would be a shift of the $V-K$ color from its typical value of 3.2 ± 0.3 for a galaxy to ~ 4.0 for the cluster. If the dark matter was smoothly distributed then the $(V-K)$ color shift in regions devoid of bright galaxies would be even more dramatic.

Previous infrared searches have constrained the content of dark matter in the halos of individual galaxies (Boughn & Saulson 1983; Boughn, Saulson, & Seldner 1981; Skrutskie, Shure, & Beckwith 1985). Those measurements showed that if a population of red/brown dwarfs is invoked in order to provide the necessary mass then 50% or more of these objects must have masses smaller than 0.085 $M_\odot$ (the lower mass limit of hydrogen burning stars, Graboske & Grossman 1971).

Our motivation for extending these observations to rich clusters of galaxies was three-fold: (1) the mass-to-light ratios of clusters of galaxies are about 10 times those of individual galaxies (i.e., mass is missing in clusters of galaxies much more so than in individual galaxies even if their inferred halos are included), so that if cold stars make up a significant fraction of the dark matter they could be more easily detected in clusters of galaxies as their infrared luminosity would be proportionally larger; (2) it is important to search for a possibly distinct form of dark matter in clusters; and (3) even if the nature of the dark matter in clusters is the same as in galactic halos, the integrated fluxes from the cores of rich clusters of galaxies include the light from many galaxies rather than that from small regions of a few individual galaxies as had been observed previously.

2. OBSERVATIONS AND DATA REDUCTION

We obtained single-aperture *J* and *K* and CCD *B*, *V*, and *R* photometry of eight positions near the centers of the Abell clusters A910, A1413, A1763, and A2218. We located the center of each cluster from the galaxy distribution on the corresponding Palomar Observatory Sky Survey red plate. For A910, A1413, and A2218 these positions were near the dominant galaxies which were chosen as the centers of these clusters. For A1763, a Bautz-Morgan class III cluster, we determined the galaxy centroid from the positions of ~ 150 member galaxies. The derived position was in good agreement with that derived by Vallée & Bridle (1982) from an X-ray image obtained with

[1] Visiting Astronomer at Kitt Peak National Observatory, National Optical Astronomy Observatories, operated by Association of Universities for Research in Astronomy, Inc., under contract with the National Science Foundation.

[2] The National Radio Astronomy Observatory is operated by Associated Universities, Inc., under cooperative agreement with the National Science Foundation.

the *Einstein* IPC. We located as well the nearest areas devoid of galaxies brighter than the Palomar E-plate limit that were large enough to acommodate our apertures, which we shall hereafter refer to as "off" positions.

2.1. *Single-Aperture Photometry*

We obtained single-aperture photometry in the J (1.25 μm) and K (2.2 μm) bands using the InSb photometer (Hermann) at the Cassegrain focus of the KPNO 1.3 m telescope on 1983 March 14, 15, and 20, April 2, 3, and 4; 1984 February 10, 12, and 13; and 1985 March 12, 13, and 14. A nutating secondary switched the beam at a rate of 10 Hz between two positions separated by about 10′. In order to eliminate offsets, we used a double-beam-switching scheme in which the target positions were alternatively compared with two reference positions on opposite sides of the target. Each of the single-switching observations lasted 1 minute. The distances of the target positions to the respective cluster centers are listed in Table 1. We used an aperture of 69″ for each target except for the A1763 off position which was observed with an aperture of 54″. We scanned the apertures along the NS and EW directions in both the target and reference positions for several beam-throws in order to determine the beam profiles. We scanned the telescope through the positions of bright stars while beam-switching in the same way as was done during the actual observations and recorded the output of the synchronous detector with a strip-chart recorder. The tracings were consistent with circular apertures and provided us with effective "beam maps."

J- and K-band KPNO infrared standard stars were observed at several zenith angles. A secant law was fitted to each night's data and the resultant atmospheric extinction removed from the data. These corrections amounted to at most 0.1 mag. Because the beam throws were large, the change in airglow due to the secant-law atmospheric contribution resulted in a small but nonnegligible contribution to the signal. Airglow was determined by monitoring the DC channel of the photometer at several zenith angles and this value was used to correct the data. These corrections were, in all cases, smaller than the standard deviations listed in Table 1; we chose to make them because they were nonrandom as well as predictible.

The resultant JK photometry for each cluster position are listed in Table 1. The quoted errors are statistical only. Other errors are estimated below.

2.2. *CCD Photometry*

We obtained BVR (Mould filterset) CCD photometry on the cores of these clusters with the No. 1 0.9 m telescope at KPNO on 1985 March 17, 19, 20, and 21 using the 348 × 512 RCA No. 1 chip with a scale of 0.″86 per pixel. The seeing was between 1.″1 and 1.″8. Each observation of a cluster in any given band consisted of a sequence of eight frames with an integration time of 5 minutes per frame. The sequence began with two observations of a "blank" area followed by four observations of the cluster center with two observations of a second blank area to end the sequence. The telescope was offset by about 30″ between each exposure of a given area, which for the observations of the cluster resulted in a diamond pattern. The cluster exposures contained both the "center" and "off" positions. The blank areas, which contained the reference positions used for the single-aperture J and K observations described above, were used to generate a "sky-flat" frame for each cluster-band observation as described below.

We observed stars of different spectral types of 10th–12th magnitude from Landolt's list of standard stars (Landolt 1983). The derived calibration constants agreed to within 0.03 mag for all bands.

We subtracted the bias level from each picture and trimmed them to a size of 316 × 508 pixels and subsequently divided them by standard dome-flats. All the exposures of blank positions were stacked in order to identify "hot" pixels (several hundred). These were then eliminated from further analysis.

The reduction of each group of exposures corresponding to one cluster in any given band then proceeded as follows. Each "blank" frame was submitted to a robust 3 σ filter (four iterations). Any region which consisted of three or more contiguous noncolinear pixels was designated an object and after determining its centroid and rms radius, all the pixels within 3.5 times the rms radius of the centroid of the object were also flagged. This was done in order to avoid contamination from the fuzz around galaxies and stars which would escape the 3 σ filtering. The four so-cleaned frames were averaged to form a "sky-flat" frame for each band and cluster. Any pixel which was not represented in two or more individual frames was designated "bad" and flagged. All eight frames were then flattened by division with the composite sky-flat. No residual structure other than objects was left in the flattened frames to 3×10^{-3} of the night sky.

The four central frames as well as both pairs of reference frames were tesselated. We first determined spatial offsets by cross-correlating overlapping frames. The x, y offsets determined in this way are accurate to within 0.2 pixel, but were rounded off to the nearest integer which was adequate for our purposes. Cosmic-ray hits were found by comparing the various measurements of any given sky position in an automa-

TABLE 1

PHOTOMETRY OF CLUSTER POSITIONS

Cluster	r[a]	B	V	R	J	K
A910	0″	17.42 ± 0.11	16.04 ± 0.09	15.30 ± 0.04	13.49 ± 0.09	12.26 ± 0.08
A910 off	78	$19.09^{+0.63}_{-0.40}$	$17.80^{+0.55}_{-0.36}$	17.05 ± 0.20	14.59 ± 0.27	13.66 ± 0.24
A1413	0	15.94 ± 0.03	14.83 ± 0.03	14.18 ± 0.01	12.40 ± 0.02	11.23 ± 0.03
A1413 off	105	$18.93^{+0.52}_{-0.34}$	$19.37^{+\infty}_{-1.02}$	$19.50^{+\infty}_{-0.86}$	>16.4[b]	$16.00^{+\infty}_{-1.01}$
A1763	30	16.92 ± 0.09	15.82 ± 0.08	15.16 ± 0.07	13.40 ± 0.06	11.89 ± 0.06
A1763 off	57	18.15 ± 0.19	17.33 ± 0.28	16.81 ± 0.20	$15.34^{+0.39}_{-0.29}$	13.70 ± 0.19
A2218	0	16.00 ± 0.03	15.32 ± 0.01	14.68 ± 0.03	12.82 ± 0.02	11.63 ± 0.02
A2218 off	52	17.45 ± 0.11	17.03 ± 0.06	16.38 ± 0.13	14.50 ± 0.21	13.65 ± 0.27

[a] Distance from nominal cluster center.

[b] Photometry gave a $-0.9\,\sigma$ value; the listed magnitude corresponds to $+1\,\sigma$.

ted way. Random checks showed this procedure to be successful. The nonoverlapping regions were discarded which resulted typically in a loss of only about 10% of the pixels. The sky level varied typically by $\pm 5\%$ during the first three nights and up to $\pm 12\%$ during the fourth night. Offsets between overlapping frames were computed by comparing the average sky level in the overlap region of the corresponding frames after excluding objects using the procedure described above (robust filtering followed by scaling of the objects found). Finally, overlapping frames were averaged.

In order to relate the *BVR* observations to the single-aperture photometry used in the *JK* measurements, we convolved the composite CCD frames with aperture masks at the positions of the main and reference IR beams. These masks were constructed to match the measured beam patterns of the (switching) infrared beams (see § 2.1). The beams were located by identifying stars in the CCD frames that corresponded to those visible to the automatic guider on the 1.3 m telescope to which the infrared beams were referred. We used positions in which several stars were visible to the guider in order to calibrate it in both orthogonal directions and used those values to refer the positions of the single aperture even in the case that only one star was visible (two cases). We believe that we know the position of the infrared apertures to within 1″.

The sky background in each mosaic was determined from the pixel intensity distribution. Histograms of number of pixels versus intensity were constructed from the data in each mosaic, after excluding the areas covered by the infrared beams. Gaussians were then fitted to these distributions and the procedure iterated to exclude pixels whose intensity exceeded the average by more than one standard deviation, in order to avoid a bias due to faint objects or the extended halos of bright objects. The mean of each fitted Gaussian was taken to be the corresponding background level of the night sky. This method provides a simple way to estimate a sky background which is largely insensitive to objects with intensities greater than the shot noise in the night sky, which is sufficiently accurate for our purposes. The sky background in the central mosaic was determined by the same method but pixels nearer than 150″ from the cluster center were excluded in order to avoid a possible contamination due to a diffuse component which might be present near the cluster center.

The light in any central beam minus the average light in the two corresponding reference beams can be readily compared to that obtained from the *JK* single-aperture photometry. These values are also listed in Table 1.

We perform this double subtraction in order to avoid the effects of potential contamination by faint objects in the "reference" positions. Of course, the photometry of the central beam is referred to the sky level in its corresponding CCD mosaic. A faint, diffuse, extended cluster halo could cause us to overestimate the sky background but we expect this bias to be small as we compute this background level more than two core radii away from the respective cluster centers. Furthermore, any such bias would lead us to underestimate the contribution of the normal stellar population in these clusters and therefore underestimate the lower limits to the mass-to-light ratio of the "dark matter" component (§ 4 below). Therefore, this bias does not affect the conclusions of this paper.

3. CLUSTER COLORS

3.1. *K Corrections*

K corrections are important because the observed clusters have redshifts between 0.14 and 0.20. These corrections depend on the spectrum of the observed light. Since our observations were confined to the cores of rich Abell clusters most of the galaxies in the beams are either elliptical or early-type spirals. Therefore, we computed *K* corrections assuming a spectrum of a typical elliptical galaxy. We used the composite elliptical spectrum of Lebofsky and Rieke (Eisenhardt 1984) in the infrared and the standard elliptical spectrum of Yee & Oke (1978) in the visible.

The infrared spectrum of a galaxy is largely independent of morphological type and so the *K* corrections computed for the *J* and *K* bands should be quite accurate. The visible spectrum on the other hand is fairly sensitive to morphological type and *K* corrections computed with an elliptical spectrum could be in considerable error especially so if late spiral galaxies contribute significantly to the observed "average" cluster light. The problem can be minimized in our case because the central wavelengths of the observed *V* and *R* bands correspond quite closely (within a few percent) to those of the *B* and *V* bands in the cluster rest frames. Equation (1) is an expression for a modified *K* correction which we use to transform the observed *R*-band magnitude into the rest frame *V*-band magnitude:

$$K_{R\to V} = 2.5 \log (1+Z) - 2.5 \log \left\{ \frac{\int S_R(\lambda) F_G(\lambda/[1+Z]) d\lambda}{\int S_V(\lambda) F_G(\lambda) d\lambda} \right\} - 2.5 \log \left[\frac{\int S_V(\lambda) F_\alpha(\lambda) d\lambda}{\int S_R(\lambda) F_\alpha(\lambda) d\lambda} \right], \quad (1)$$

where $S_R(\lambda)$ characterizes the *R* passband, $S_V(\lambda)$ characterizes the *V* passband, $F_G(\lambda)$ is the standard spectrum of an elliptical galaxy and $F_\alpha(\lambda)$ is the spectrum of α-Lyr, i.e., a zero-magnitude A0V star. Since we are transforming from one band to another it is necessary to refer all fluxes to those of a standard zero-magnitude star. To the extent that $S_R(\lambda) \approx S_V(\lambda/[1+Z])$, it is clear that the *K* correction of equation (1) is independent of the shape of the standard galaxy spectrum, $F_G(\lambda)$. The filter-detector response curves, $S(\lambda)$, of the bands were obtained from KPNO filter tracings and the measured CCD quantum efficiency. The InSb photometer quantum efficiency was taken from typical data provided by the manufacturer. Even though the resultant filter-detector response curves are somewhat uncertain, we believe that such uncertainty is preferable to those due to the spectra of the observed sources.

Table 2 lists the standard *K* corrections for the *J* and *K* bands as well as the modified *K* corrections from equation (1) for $V \to B$ and $R \to V$. It is difficult to estimate *K* corrections for the observed *B* band as in the cluster rest frame this band falls in the ultraviolet part of the spectrum which is highly dependent on morphological type and galaxy orientation. For this reason we do not include the observed *B*-band data in the following analysis.

In order to check the accuracy of the modified *K* corrections, $R \to V$ and $V \to B$, we computed their values for hypothetical spiral galaxies of all morphological types emitting at the clusters' redshifts. The errors induced in the corrected $(B-V)$

TABLE 2

K CORRECTIONS

Cluster	*K*	*J*	$R \to V$	$V \to B$
A910.....	−0.43	−0.05	−0.32	−0.50
A1413.....	−0.32	−0.07	−0.40	−0.63
A1763.....	−0.41	−0.06	−0.34	−0.55
A2218.....	−0.38	−0.06	−0.35	−0.56

TABLE 3

CORRECTED COLORS

Cluster	$B-V$	$V-K$	$J-K$
A910	0.92 ± 0.15	2.93 ± 0.14	0.85 ± 0.17
A910 off	$0.93^{+0.60}_{-0.43}$	3.28 ± 0.33	0.55 ± 0.38
A1413	0.89 ± 0.12	3.03 ± 0.12	0.92 ± 0.12
A1413 off	...	...	...
A1763	0.87 ± 0.16	3.20 ± 0.15	1.16 ± 0.14
A1763 off	0.73 ± 0.36	3.04 ± 0.30	$1.29^{+0.45}_{-0.36}$
A2218	0.85 ± 0.12	3.02 ± 0.12	0.87 ± 0.12
A2218 off	0.86 ± 0.18	2.70 ± 0.32	0.53 ± 0.36
Average E/S0	0.93 ± 0.05	3.18 ± 0.21	0.82 ± 0.07

colors were from 2 to 3 times smaller than those incurred from using standard K corrections. We estimate that the uncertainties in the values listed in Table 2 are ≤ 0.05 mag.

All of these clusters lay at large Galactic latitude, $b \geq 40°$, so no correction was made for Galactic extinction.

3.2. *Corrected Colors*

The corrected colors for the cluster positions are listed in Table 3 along with the average colors obtained from a survey of nearby E/S0 galaxies (Frogel et al. 1978; Persson, Frogel, & Aaronson 1979; Aaronson, Persson, & Frogel 1981; Aaronson 1977). The survey colors were corrected slightly (≤ 0.1 mag) to take into account the radial color gradients reported by Frogel et al. (1978). All colors were corrected to one de Vaucouleurs radius. The errors listed are a quadrature combination of the statistical errors and 0.08 mag which accounts for any uncertainties in calibration and the K corrections discussed above. The uncertainties listed in the last row reflect the spread in the colors (standard deviation) of the survey galaxies.

Figure 1 is a color-color diagram of the corrected $V-K$, $J-K$ colors of seven cluster positions (no light was detected from the A1413-off position). The closed contour contains 90% of the E/S0 galaxies in the photometric surveys mentioned above. It is clear from Table 3 and Figure 1 that the colors of the integrated light from these clusters are consistent with those of the luminous parts of nearby galaxies. If the dark matter does make a significant contribution to cluster light, such contribution evidently has a stellar luminosity function comparable to that of the luminous portions of galaxies.

3.3. *Contamination by Stars and Galaxies*

We estimate the effect of background galaxies using the galaxy number-counts of Tyson & Jarvis (1979) and Kron (1980). We convert these into the appropriate photometric bands taking into account the corresponding K corrections. The expected contribution of background galaxies is either smaller than 5% of the measured signal or smaller than the noise in all cases. Similar calculations for stars, using the predicted star counts of Bahcall & Soneira (1981), show these to be even less important. We conclude that contamination by foreground and/or background objects cannot significantly alter the conclusions of this paper.

4. DISCUSSION

4.1. *Cluster Masses*

In order to determine the mass-to-light ratios of the clusters, the projected surface mass densities must be estimated as a function of cluster position. Assuming an isothermal King distribution (King 1972), the surface-density is, to a good approximation,

$$\sigma(r) = \frac{2\rho_0 r_c}{(1 + r^2/r_c^2)} \qquad (2)$$

where r_c is the core radius, the central density is $\rho_0 = 9v_r^2/4Gr_c^2$ and v_r^2 is the line-of-sight velocity dispersion. This model assumes that the dark matter is distributed like the galaxies. As was pointed out by Bailey (1982), the total mass of the cluster

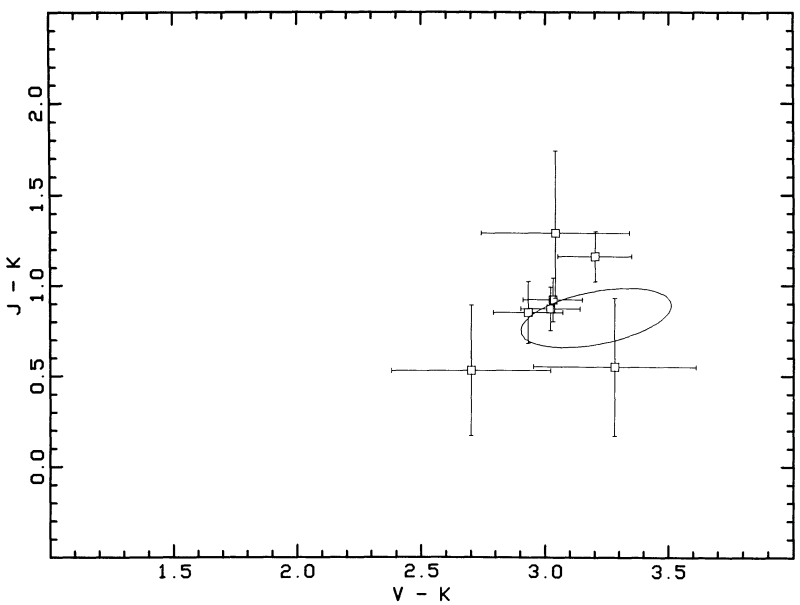

FIG. 1.—Color-color diagram for the observed Abell clusters. The three points with largest error bars correspond to the off positions (those away from the cluster centers). No significant luminosity was detected for the A1413 off position so it is missing from this plot. The contour contains 90% of the E/S0 galaxies in the survey of Frogel et al. (1978), see text.

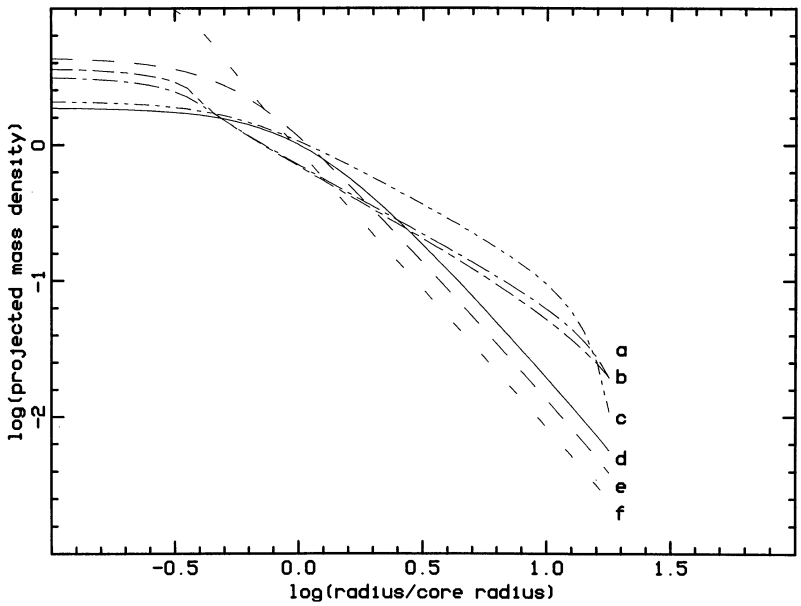

FIG. 2.—Surface density profiles for dark matter models of the Coma cluster. (*a*) $q = 1$, $b = r_c/16$; (*b*) infinite isothermal sphere; (*c*) $q = 1$, $b = r_c/2$; (*d*) $q = 3/2$, $b = r_c$ (standard King profile); (*e*) $q = 3/2$, $b = r_c/2$; (*f*) $q = 3/2$, $b = r_c/8$. The curves are all normalized to a central density $\rho_0 = 9v_r^2/4\pi G r_c$ (see eq. [2]).

can vary significantly by relaxing this restriction. However, the surface density near the central part of the cluster does not show this great variation. For example, we have considered models for the Coma cluster in which the dark matter is distributed according to $\rho_d \propto (1 + r^2/b^2)^{-q}$. Following Bailey (1982) we picked values of b and q which differed from the canonical values of r_c and 3/2 yet still satisfied hydrostatic equilibrium with the velocity dispersion profile obtained by Kent & Gunn (1982). All the models were truncated between $20r_c$ and $25r_c$. The resultant surface density profiles were averaged over a disk of radius $3r_c/8$ which corresponds roughly to the 1′ aperture used in our observations. Figure 2 is a plot of five such profiles and, in addition, of the profile of an infinite isothermal sphere, i.e., $\rho_d \propto 1/r^2$. For $r \leq 3r_c$ it is clear that the projected surface density of the dark matter is fairly insensitive to its radial distribution except for the centrally condensed models which show a significant increase in surface density near the center, $r \leq 0.3r_c$. These models all assumed isotropic velocity distributions; however, relaxing this condition has little effect on surface density (Kent & Gunn 1982). Departures from spherical symmetry can be expected to have a greater effect. It was for this reason that we picked clusters which appeared symmetrical on the Palomar prints and had symmetrical X-ray profiles (when they were available).

We adopt a value of $0.2h^{-1}$ Mpc for the cluster core radii[3] which is typical for rich clusters (Sarazin 1986). This assumption is acceptable since the surface mass density at distances near one core radius is not very sensitive to the value of the core radius. For example, the surface density given by equation (1) at $r = 0.2$ Mpc changes by only 25% if r_c is doubled from 0.2 Mpc to 0.4 Mpc. Total cluster masses, on the other hand, are roughly proportional to the adopted core radii.

The remaining quantity required to determine the surface mass densities is the line-of-sight velocity dispersion, v_r^2. Although velocity dispersions have not been published for the clusters in this study, all are rich Abell clusters (richness class ≥ 3) which typically have velocity dispersions in excess of 1000 km s^{-1} (Bahcall 1981). In addition, X-ray luminosities for the clusters have been determined from *Einstein* observations (Jones et al. 1979; Vallée & Bridle 1982; Abramopoulos & Ku 1983). We have used the correlation between X-ray luminosity and velocity dispersion (Quintana & Melnick 1982) to arrive at the estimates in Table 4. These are probably good to 10%. A preliminary estimate of the velocity dispersion of A2218 ($\sim$1100 km s^{-1}), kindly communicated to us by H. Spinrad is indeed consistent with that determined from its X-ray luminosity (1200 km s^{-1}) to within our estimated 10% uncertainties.

We have computed the projected masses which lay within the apertures of the eight measured positions assuming isothermal King profiles and the above line-of-sight velocity dispersions. These are listed in Table 5 along with the B, V, J, and K mass-to-light ratios expressed in solar units. We computed the luminosities assuming an open ($q_0 = 0$) cosmology. A flat universe ($q_0 = 0.5$) would imply mass-to-light ratios about 10% larger than those listed.

4.2. *Dark Matter Constraints*

Let us derive an upper limit to the contribution of red dwarfs to the dark matter by computing the maximum mass which could be present in the form of late M dwarfs ($M = 0.1\ M_\odot$) without resulting in galaxy colors which were redder than

TABLE 4

LINE-OF-SIGHT VELOCITY DISPERSIONS INFERRED FROM X-RAY LUMINOSITIES

Cluster	σ_v (km s^{-1})
A910	1130
A1413	1230
A1763	1400
A2218	1200

[3] We adopt the usual convention $h \equiv H_0/(100\ \text{km s}^{-1}\ \text{Mpc}^{-1})$.

TABLE 5

MASSES AND MASS-TO-LIGHT RATIOS

Cluster Positions	Mass ($10^{13}\ h^{-1}\ M_\odot$)	$(M/L)_B\ h^{-1}$	$(M/L)_V\ h^{-1}$	$(M/L)_J\ h^{-1}$	$(M/L)_K\ h^{-1}$
A910	3.60	217	169	34	42
A910 off	2.20	670	517	57	93
A1413	2.50	117	94	18	21
A1413 off[a]	1.50	>1790	>3440	>440	>409
A1763	4.65	280	229	48	44
A1763 off	2.31	560	520	142	117
A2218	2.73	123	102	19	23
A2218 off	2.27	492	405	75	125

[a] The *B*-, *V*-, and *K*-band upper limits are derived from 1 σ upper limits to the luminosity, while the *J*-band upper limit corresponds to a luminosity equal to 1 σ.

observed. The $V-K$ color is especially useful in this respect since it is, a sensitive probe to red dwarfs while not being too sensitive to galaxy morphological type. We adopt as the spectrum of a canonical M8 dwarf that of W359 (Greenstein et al. 1970). Since M8 dwarfs have different *K* corrections than galaxies we proceed as follows. The light of the hypothetical population of red dwarfs is *K*-corrected to the observer's frame and subtracted from the observed luminosity. The remaining luminosity is then *K*-corrected back to the cluster frame assuming it has the canonical galaxy spectrum. If the corrected $(V-K)$ color of the cluster is so blue that its 1 σ upper limit falls below 2.90, the lower extreme of the contour of Figure 1, then the hypothesized red dwarf population is considered to be inconsistent with observations. We take this to be an upper limit to the contribution of red dwarfs to the dark matter. Table 6 lists these upper limits in terms of a fraction of the dark matter. The limit derived for the off position of A1413 was calculated by attributing to the dark matter all of the light allowed by the 1 σ upper limit to the *K*-band luminosity.

A lower limit to the mass-to-light ratio should be quoted at a wavelength of 1.9 μm since this is roughly the wavelength in the rest frame that corresponds to the light we observe in the *K* band. However, since the reason to derive mass-to-light ratios in the present context is for comparison to that of late dwarfs we adopt as lower limits to the *K*-band mass-to-light ratio that of W359 ($\sim$20) divided by the upper limits to fractional composition of such stars which are listed in Table 6. These lower limits to the *K*-band mass-to-light ratios are listed in the last column in Table 6. For comparison, $(M/L)_K$ for VB10, one of the faintest known main-sequence stars is about 34 (Greenstein et al. 1970) if one assumes its mass is 0.085 $M_\odot$.

TABLE 6

LIMITS ON THE FRACTION OF DARK MATTER IN THE FORM OF M8 DWARFS

Cluster	Dark Matter in M8 Dwarf	Equivalent $(M/L)_K$
A910	$6.9h^{-1}$%	$290h$
A910 off	$10.3h^{-1}$%	$194h$
A1413	$19.4h^{-1}$%	$103h$
A1413 off	$4.9h^{-1}$%	$409h$
A1763	$15.4h^{-1}$%	$130h$
A1763 off	$5.8h^{-1}$%	$345h$
A2218	$17.0h^{-1}$%	$118h$
A2218 off	$1.7h^{-1}$%	$1176h$

It is clear from Table 6 that the data taken at the off-center positions provide the strongest constraints on the mass-to-light ratio. These areas were carefully chosen to avoid large galaxies. It is obvious that these underluminous areas have large mass-to-light ratios under the assumption that the dark matter is distributed smoothly throughout the cores of these clusters. This is reasonable since inside the cluster cores the intergalactic spacings are only a few tens of kiloparsecs, so if the dark matter was originally in the halos of individual galaxies it would have long been stripped and smoothed out on a time scale of a few billion years. On the other hand, if the dark matter is contained within individual galaxies, such massive objects would have collapsed to the center through dynamical friction (Sarazin 1986) which is clearly not the case. Uncertainties in the above analysis preclude us from placing undue importance on the individual entries in Table 6. However, taken as a whole they provide important constraints on the dwarf-stellar component of the dark matter. For example, if we assume that $5h^{-1}$% of the dark matter consists of M8 dwarfs then the corrected colors of the cluster galaxies are as shown in Figure 3. It is clear that while the central cluster positions have colors still consistent with normal galaxies, two of the three off-center positions do not. This conclusion is strenthened by the A1413 off position which is not plotted on the figure but is also inconsistent with a $5h^{-1}$% dwarf contribution (see Table 6).

The above argument on the distribution of dark matter notwithstanding, if one assumes that dark matter is associated with galaxies then only the center cluster positions should be considered. Figure 4 is a plot of the colors of the central cluster positions after having been corrected for a $15h^{-1}$% dwarf contribution to the dark matter. Again the inconsistency with the colors of normal galaxies is evident. We consider this to be an excessively conservative lower limit.

Henriksen & Mushotzky (1985) have argued that a large fraction of the total dynamical mass of a rich cluster is in the form of ionized hydrogen, up to 63% in the case of A2029. This follows primarily from their observation that hydrogen is more extended than the usual dynamic dark matter models. Again this is not the case for the projected mass density near a core radius. Using their model for the distribution of hydrogen we conclude that in A2029 only 9% of the projected mass density near one core radius is accounted for by ionized hydrogen. A

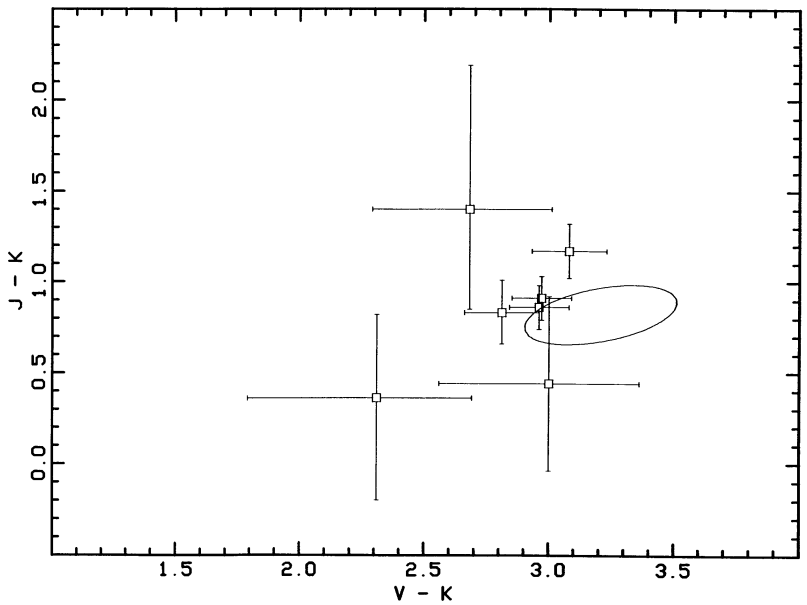

FIG. 3.—Color-color diagram for the observed clusters corrected for a population of M8 dwarfs which would constitute $5h^{-1}$% of the dark matter. See Fig. 1 and text.

similar computation for the Coma cluster gives 8%. Therefore, even if Henriksen & Mushotzky are correct, the limits in Table 6 would change by less than 10% if we excluded the ionized-hydrogen component of the dark matter.

4.3. *The Dark Matter Function*

Hegyi & Olive (1986) have argued against placing so much mass in small objects on the grounds that this would require a steeper initial mass function than is consistent with galaxy colors. One must be cautious, however, in using observations of what are essentially objects of mass $\sim M_{\odot}$ (giant and main-sequence stars) to make inferences about objects which are from one-tenth to one-thousandth times less massive. If the dark matter is composed of a population of substellar objects, then it is clear that this population must have evolved from an initial mass function which is distinct from that of the luminous parts of galaxies; otherwise, it would be hard to explain the great variation of mass-to-light ratios with galactic position. If dark matter is indeed produced according to a power-law mass function, then either (1) the slope of that mass function must increase, or (2) the upper cutoff mass must decrease (and the amplitude increase), or (3) the lower cutoff mass must decrease dramatically as one moves from the centers of galaxies out to their halos and into the intergalactic region. We now investigate these possibilities.

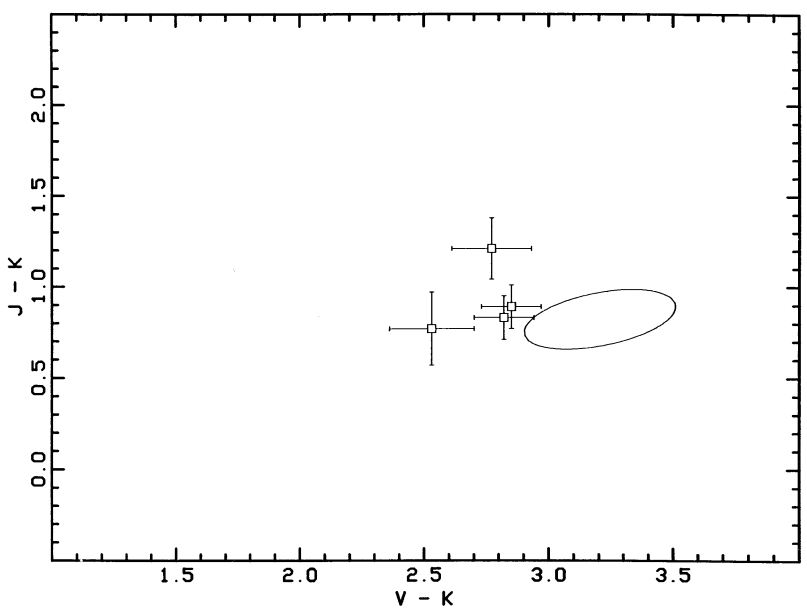

FIG. 4.—Color-color diagram for the central cluster positions corrected for a population of M8 dwarfs which would be $15h^{-1}$% of the dark matter. See Fig. 1 and text.

The minimum mass that allows objects to collapse gravitationally has been estimated to be $M \geq 0.004\ M_\odot$ (about 4 times the mass of Jupiter); although these calculations are uncertain (Low & Lynden-Bell 1976; Silk 1982; Palla, Salpeter, & Stahler 1983). With a sufficiently steep mass spectrum it could still be possible to hide the necessary mass in objects in this mass range.

Following Hegyi & Olive we consider a power-law mass function of the form, $\Phi(M) = A\ M^{-(1+x)}$, truncated at the upper end at $M = 0.75\ M_\odot$, which is taken to be the mass of a giant star in a typical elliptical galaxy, and at the lower end at $M = 0.004\ M_\odot$ (see above). Using the spectral data of Tinsley & Gunn (1976) for giant and dwarf stars, Hegyi & Olive solved for the expected K-band mass-to-light ratio as a function of the slope parameter x. The $5h^{-1}\%$ limit on the red-dwarf content of dark matter derived above corresponds to a K band mass-to-light ratio of $400h$ in solar units. According to their analysis, $(M/L)_K \geq 400$ implies $x \geq 2.4$. Using the stellar synthesis models of Tinsley & Gunn (1976), observations currently constrain $x \leq 1$. It should be emphasized that these two apparently exclusive constraints on x are only an indication of how much x would have to increase in underluminous regions in order to account for the increased mass-to-light ratio.

Now consider a mass function with $x = 1$ and a lower cutoff mass of $M = 0.004\ M_\odot$. Again, if $(M/L)_K \geq 400$, the analysis of Hegyi & Olive implies that the upper mass cutoff is less than $0.1\ M_\odot$. Finally, if we assume that $x = 1$ and an upper end cutoff $M = 0.75\ M_\odot$, then no lower cutoff mass is consistent with our measured M/L limits. These results are only an indication of the kind of constraints that a distribution of substellar objects must satisfy.

5. CONCLUSIONS

Even at $\lambda = 2\ \mu$m, the dark matter in clusters of galaxies is exceedingly dark—a factor of 10 darker than the faintest main-sequence stars. If dark matter is composed of an extension of the main sequence to objects too small to burn hydrogen, i.e., brown dwarfs, then 95% or more of the matter consists of objects with masses smaller than $0.1\ M_\odot$. According to some theoretical arguments, the smallest objects that can form gravitationally are only 25 times smaller than this. Such substellar objects would be virtually impossible to detect directly (Liebert & Probst 1987). However, objects as small as $10^{-4}\ M_\odot$ may be observable as gravitational lenses (Gott 1981). The smallest objects which could survive for a Hubble time without evaporating have masses of $\sim 10^{-14}\ M_\odot$ (Peebles 1971). It is quite possible to hide as much (baryonic) mass as needed in such objects although it is difficult to understand how such objects can form.

We acknowledge helpful discussions with Jay Gallagher, Eric Greisen, Jeff Kuhn, Richard Larson, Tony Letai, Ed Loh, Ron Probst, and Earl Spillar. We thank the staff at KPNO for their support with these observations. Part of this work was done while one of us (J. M. U.) enjoyed the hospitality of the Radio Astronomy Lab at UC Berkeley. This research was supported in part by the National Science Foundation.

REFERENCES

Aaronson, M. 1977, Ph.D. thesis, Harvard University
Aaronson, M., Persson, S. E., & Frogel, J. A. 1981, ApJ, 245, 18
Abramopoulos, F. G., & Ku, W. H.-M. 1983, ApJ, 271, 446
Bahcall, J. N., & Soneira, R. A. 1981, ApJS, 47, 357
Bahcall, N. A. 1981, ApJ, 247, 787
Bailey, M. E. 1982, MNRAS, 201, 271
Boughn, S. P., & Saulson, P. R. 1983, ApJ, 265, L55
Boughn, S. P., Saulson, P. R., & Seldner, M. 1981, ApJ, 250, L15
Einsenhardt, P. R. M. 1984, Ph.D. thesis, University of Arizona
Faber, S. M., & Gallagher, J. S. 1979, ARA&A, 17, 135
Frogel, J. A., Persson, S. E., Aaronson, M., & Mathews, K. 1978, ApJ, 220, 75
Gott, J. R. 1981, ApJ, 243, 140
Graboske, H. C., Jr., & Grossman, A. S. 1971, ApJ, 170, 363
Greenstein, J. L., Neugebauer, G., & Becklin, E. E. 1970, ApJ, 161, 519
Hegyi, D. J., & Olive, K. A. 1986, ApJ, 303, 56
Henriksen, M. J., & Mushotzky, R. F. 1985, ApJ, 292, 441
Jones, C., Mandel, E., Schwarz, J., Forman, W., Murray, S. S., & Harnden, F. R., Jr. 1979, ApJ, 234, L21
Kent, S. M., & Gunn, J. E. 1982, AJ, 87, 945
King, I. R. 1972, ApJ, 174, L123
Kron, R. G. 1980, ApJS, 43, 305
Landolt, A. U. 1983, AJ, 88, 439
Liebert, J., & Probst, R. G. 1987, ARA&A, 25, 473
Low, C., & Lynden-Bell, D. 1976, MNRAS, 176, 367
Palla, F., Salpeter, E. E., & Stahler, S. W. 1983, ApJ, 271, 632
Peebles, P. J. E. 1971, Physical Cosmology (Princeton: Princeton University Press), p. 110
Persson, S. E., Frogel, J. A., & Aaronson, M. 1979, ApJS, 39, 61
Quintana, H., & Melnick, J. 1982, AJ, 87, 972
Sarazin, C. L. 1986, Rev. Mod. Phys., 58, 1
Silk, J. 1982, ApJ, 256, 514
Skrutskie, M. F., Shure, M. A., & Beckwith, S. 1985, ApJ, 299, 303
Tinsley, B. M., & Gunn, J. E. 1976, ApJ, 203, 52
Tyson, J. A., & Jarvis, J. F. 1979, ApJ, 230, 153
Vallée, J. P., & Bridle, A. H. 1982, ApJ, 253, 479
Yee, H. K. C., & Oke, J. B. 1978, ApJ, 226, 753
Zwicky, F. 1933, Helvetica Phys. Acta, 6, 110